RSC Advances

ROYAL SOCIETY OF CHEMISTRY

www.rsc.org/advances

Binding of Hemoglobin to Ultrafine Carbon Nanoparticles: A Spectroscopic Insight into a Major Health Hazard

Biswadip Banerji,*[a] Sumit Kumar Pramanik [a], Uttam Pal [b], Nakul Chandra Maiti [b]

[a] *Department of Chemistry and* [b] *Department of Structural Biology and Bioinformatics; CSIR-Indian Institute of Chemical Biology; 4, Raja S.C. Mullick Road, Kolkata, Country. India-700032; Fax: (+) 91 33 24735197, 91 33 24723967; Tel: (+) 91 33 24995709*

E-mail: biswadip.banerji@gmail.com

Abstract

The carbon nanoparticles (CNPs) are light and easily absorbed into different parts of organs of the human body. They are suspended particulate matters of respirable sizes. In the atmosphere ultrafine CNPs are known to be generated mainly from the combustion of fuels and have been reported to be a major contributor to the induction of cardiopulmonary diseases. In the third world country these diseases are more prevalent because of its more abundance in the air. Different nanostructured materials are when exposed to the human body they can easily enter into the body through the lungs or other different organs and tissues. In the laboratory ultrafine carbon nanoparticles were synthesized and confirmed its structure by DLS experiments, TEM and AFM imaging studies. Their interactions with hemoglobin (Hb) and myoglobin (Mb) were studied using fluorescence spectroscopy. The results indicate a remarkably strong interaction between carbon nanoparticles and Hb (or Mb). The temperature dependent steady sate fluorescence spectroscopy showed exothermic binding of Hb to CNPs, which is favored by enthalpy and entropy changes. Circular dicroism study also indicated significant change of protein secondary structure and partial unfolding of the helical conformation. These findings are highly important in understanding the interactions between CNPs and Hb (or Mb) which might help to clarify the potential risks and undesirable health hazards associated with carbon nanoparticles in a better way.

Keywords

Carbon nanoparticles, Health hazard, Fluorescence, Circular dichroism.

Introduction

The domain of nanotechnology is rapidly increasing, and today there are more than 1,500 nanoproducts on the market.[1-2] The different nanostructured materials like nanotubes,[3] nanoparticles,[2] nanocages,[4] nanopowders,[5] nanowires,[6] nanoshell,[7] nanorods,[8] nanofibers,[9] quantum dots,[10] fullerenes,[11] liposomes,[12] neosomes,[13] nanoclusters,[14] nanomesh,[15] nanocrystals,[16] nanofilm[17] and nanocomposites[18] are internationally produced in bulk quantities due to their wide potential applications in skincare and consumer products, healthcare, photonics, electronics, biotechnology, engineering products, pharmaceuticals, drug delivery, and agriculture etc. When different nanostructured materials are exposed to the human body they can easily enter into the body through the lungs or other different organs and tissues such as the brain, liver, kidney, heart, colon, bone, blood via food, drink, and medicine.[19-22] These nanomaterials may cause cytotoxic effects, e.g., deformation and inhibition of cell growth leading to various diseases in humans and animals. The toxicity and interactions of these nanomaterials with biological systems largely depend upon their physicochemical properties, such as size, concentration, solubility, chemical composition and stability.[23-26]

Carbon nanoparticles (CNPs) are a popular nanomaterial because of its interesting properties; those actually are desirable in many industrial purposes.[27] CNPs have physicochemical properties which are already in use in the commercial, environmental, and medical sectors.[28-32] However, with a diameter in the nanoscale, this extremely small particle may constitute a health risk.[33]

Studies of particle emission from a steady burning single paraffin wax candle found the size of particles produced to be around 30 nm in diameter.[34] And the concentrations of particles emitted from a pure wax candle and a scented candle in a chamber and found the

concentrations of particles to be 240 000 particles cm^{-3} and 69 000 particles cm^{-3} respectively.[35] The CNPs are very light and very easily enter in the working environment they are suspended particulate matter of respirable sizes.[36] For this reason these CNPs could pose an occupational inhalation exposure hazard. CNPs of size <2.5 micron are found in combustion streams of methane, propane, butane and natural-gas flames of typical stoves. Both in case of indoor and outdoor fine particle samples contain a significant fraction of CNPs. It is already reported that CNPs were more toxic than quartz, and causes occupational health hazard if it is chronically inhaled.[37] Environmental fine CNPs are known to be generated mainly from combustion of fuels, and has been reported to be a major contributor to the induction of cardiopulmonary diseases by pollutants.[38] Therefore, CNPs from manufactured and combustion sources in the environment could have adverse effects on human health.

The carbon nanotubes (CNT) are known to have a wide range of biomedical applications but the importance of nanoparticle–protein interactions are not stressed enough.[39] Although systemic interactions of CNTs with various plasma protein have been reported. However, despite the fact that CNPs can penetrate plasma membrane, the knowledge of the effect of CNPs on blood corpuscular protein, haemoglobin is still obscure.[40-44] Inhalation of CNPs from the environment directly exposes them to our blood circulatory system.[42-44] Therefore, to know the interaction between CNP and the oxygen transporter protein, hemoglobin, is essential to clarify the impact of CNPs on human health. Here, in this paper we present a detailed study on the interaction of haemoglobin with CNPs by using fluorescence spectroscopy and circular dichroism spectroscopy (CD). For a better understanding, we have used myoglobin alongside hemoglobin in this study, which can be thought of as a monomeric unit or hemoglobin. Myoglobin is functionally similar to hemoglobin and shares similar

structural fold despite the dissimilarities in amino acid composition, thus, provides a deeper insight into the effect of CNPs on hemoglobin.

Materials and method

Materials

Human hemoglobin and myoglobin were purchased from Sigma–Aldrich (USA). Carbon soot, acetone, TrisHCl and nitric acid were also purchased from Sigma-Aldrich. All the samples were prepared in 20 mM Tris HCl buffer of pH 7.4 for CNP-protein interaction studies. Deionized and triple distilled water was used for preparing buffer solution that was passed through 0.22 μm pore size Millipore filters (Millipore India Pvt. Ltd., Bangalore, India). Carbon coated copper grid for TEM study was purchased from Allied Scientific Product, USA. ASTM V1 Grade Ruby Mica sheet for AFM study was purchased from Micafab India Pvt. Ltd., Chennai, India.

Synthesis of carbon nanoparticles (CNPs) [45]

100 mg carbon soot was added to 60 mL of 6 (M) Nitric acid in a 25 mL three necked flask. The reaction mixture was then refluxed at 100^{o}C for 10 hours under stirring condition. After that a black solution was obtained. The solution was then centrifuged at 2000 rpm for 15 minutes to separate out the unreacted carbon soot. In subsequent step, the aqueous solution was mixed with acetone and then centrifuged at 30000 rpm for 20 minutes and the black precipitate was obtained. The precipitate was washed in 5-10 mL water to remove the excess nitric acid. Then the precipitate was dried and the weight was measured. Then it was dissolved in appropriate amount of buffer to obtain the desired concentration. The pH of the final suspension was adjusted to 7.4 and this suspension was used for further experiments.

Dynamic light scattering (DLS)-based zeta-potential measurements

To obtain an idea about the size distributions of CNPs, DLS experiments (model: Zetasizer Nano Z, Malvern Instruments Ltd, United Kingdom) were carried out with its aqueous suspension. The scattered lights were collected at a 90º angle. Data were acquired and analyzed by Precision Deconvolve program. For a typical DLS experiment, 200 μL of a sample solution was slowly pipetted into a clean quartz micro-cuvette.

TEM sample preparation and imaging

For TEM imaging, 20 μL of the nanoparticle solution was placed on a 300-mesh carbon coated copper grid and the excess samples were removed cautiously by tissue paper. It was finally dried and the images of the resulting nanoparticle solutions were recorded on Tecnai G2 Spirit Bio TWIN (Type: FP5018/40) at an acceleration voltage of 80 kV.

AFM sample preparation and imaging [45]

Twenty microliters of the nanoparticle solution was deposited onto freshly cleaved muscovite Ruby mica sheet for 5 to 10 min. After 10 min, the sample was dried using a vacuum dryer. AAC-mode atomic force microscopy was performed using a Pico Plus 5500 AFM (Agilent Technologies, Inc., Santa Clara, CA, USA) with a piezo scanner maximum range of 9 μm. Microfabricated silicon cantilevers of 225 μm in length with a nominal spring force constant of 21 to 98 N/m were used from nanosensors. Cantilever oscillation frequency was tuned into resonance frequency. The cantilever resonance frequency was 150 to 300 kHz. The images (512 × 512 pixels) were captured with a scan size between 0.5 and 5 μm at the scan speed rate of 0.5 rpm. The images were processed by flattening using Pico view software (Molecular Imaging Inc., Ann Arbor, MI, USA). The image presented in this paper was

derived from the original data. Length, height, and width were measured manually using Pico view software.

Fluorescence spectroscopy

The steady-state fluorescence spectra were recorded with a Perkin Elmer LS-45 spectrofluorophotometer at 25 ^{o}C. The samples were excited at 280 nm wavelength and emission spectra were recorded over the emission range of 300-450 nm. In all the cases the excitation and emission slit widths were kept at 5 nm each. The intrinsic fluorescence of protein was measured in the presence and in the absence of the CNPs. Intrinsic fluorescence of Mb and Hb originated from both the Trp and Tyr. Hb contains 6 Trp and 12 Tyr whereas Mb contains 2 Trp and 2 Tyr. The fluorescence of the protein was quenched in the presence of the CNPs. The quenching experiment was carried out simply by adding small aliquots of concentrated CNP solution to hemoglobin or myoglobin solution taken in 1 cm path length quartz cuvette. The protein concentration was kept at 0.5 μM and the CNP concentration was varied from 0.5 μM to 5 μM. The optical density of the solution at the excitation wavelength was kept less than 0.05. Small error due to dilution upon addition of the CNPs was neglected. Fluorescence intensities at emission maximum were recorded as a function of ligand concentration. To derive the binding parameters, obtained data were analyzed using modified Stern–Volmer equation (equation 1).

$$F_0/\Delta F = 1/fK[Q] + 1/f \quad \ldots\ldots(1)$$

Where F_0 is the fluorescence intensity in the absence of an external quencher, ΔF is the difference in fluorescence in the absence and presence of the quencher at concentration [Q], K is the Stern–Volmer quenching constant, and f *is* the fraction of the initial fluorescence which is accessible to the quencher. Binding dissociation constant, K_d, was measured as the reciprocal of K.

Temperature dependent fluorescence quenching was performed to obtain the K_d values as a function of temperature and the thermodynamic parameters of binding was determined from it fitting van't Hoff equation (equation 2) to the data.

$$\ln K = -\Delta H°/RT + \Delta H°/R \quad \text{.....(2)}$$

Where K is the equilibrium constant (here the Stern–Volmer quenching constant) of binding at corresponding temperature T, and R is the gas constant. The equation gives the standard enthalpy change (ΔH°) and standard entropy change (ΔS°) on binding. The free energy change (ΔG°) has been estimated from the following relationship (equation 3):

$$\Delta G° = \Delta H° - T\Delta S° \quad \text{.....(3)}$$

CD spectroscopy

The conformational changes in the secondary and tertiary structures of hemoglobin and myoglobin on binding of CNPs were studied using a Jasco J-810 spectrometer at 25 ˚C. The CD spectra of Hb and Mb were finally obtained by averaging five successive scans recorded at a scan speed of 50 nm min^{-1} and subtracting the appropriate blanks (tris buffer) from these spectra. For Hb and Mb proteins the changes in the far UV-CD spectra (200–250 nm) provide insights about the changes in the secondary structure of the proteins. The protein concentrations were 0.75 μM for Hb and 3.0 μM for Mb.The results are expressed in terms of mean residual ellipticity (MRE) in ◦ cm^2 $dmol^{-1}$ according to the equation given below.[46]

$$MRE = \frac{\text{observed CD (mdeg)}}{C_p \text{nl} \times 10}$$

Where Cp is the molar concentration of the protein, n is the number of amino acid residues (n = 574 for Hb and 154 for Mb) and l is the path length (here l = 0.1 cm, i.e. the path length of the cuvette used). Helical content of free and bound protein has been eventually evaluated from the MRE values at 208 nm using equation given below[46]

$$\alpha - helix\ \% = \left[\frac{-MRE_{208} - 4000}{33000 - 4000}\right] \times 100$$

Results and discussion

DLS study

The results of DLS experiment showed that the mean particle sizes of CNPs are of 20.17 nm. The zeta potential distributions of CNPs are with negative charge -39.1mV in water, which is sufficient to keep the particles from interacting with each other and therefore maintain a stable particle size of the sample. The resulting negative charges in CNPs tagged are attributed to negative surface charge on it.

TEM and AFM imaging

The transmission electron microscopy (TEM) images of the prepared CNPs have a spherical morphology with relatively regular size of diameter ~20.0 nm. They are nearly almost uniform in nature. The atomic force microscopy (AFM) study was in good agreement with the TEM results which showed the average size of have a spherical morphology with relatively regular size of diameter ~22.0 nm.

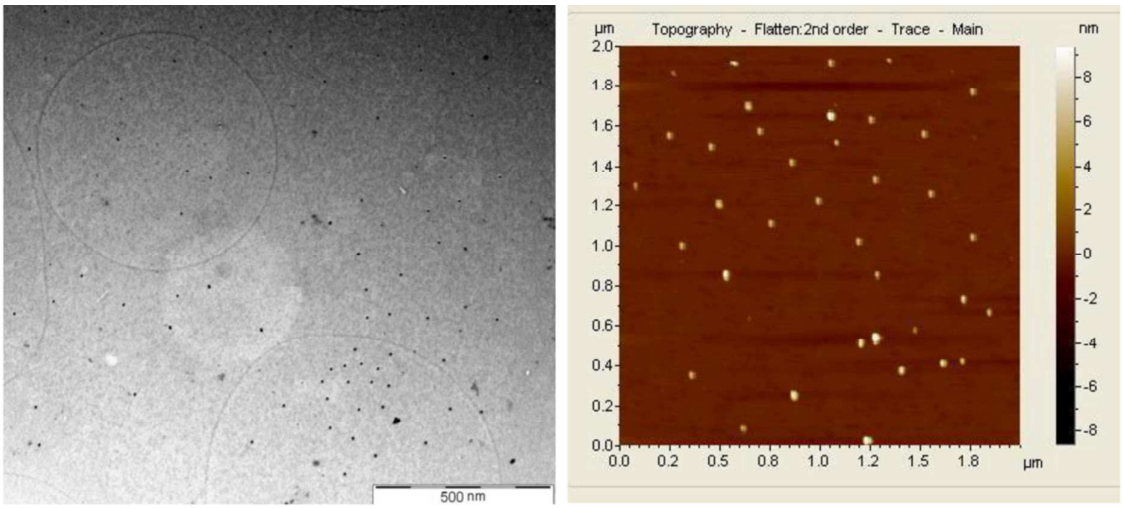

Figure 1 TEM (A) and AFM (B) image of synthesized ultrafine CNPs.

Fluorescence spectroscopy

The fluorescence spectra of Hb/Mb were measured in the presence and absence of CNPs. Hb shows a strong fluorescence with a emission peak at ~353 nm (Figure 2A). Mb with showed similar fluorescence behavior, however, with emission peak at ~330 nm. The CNPs showed no intrinsic fluorescence in the experimental buffer solution. However, the presence of CNPs in the solution effectively reduced fluorescence yield of Hb/Mb. For both the Hb and Mb, the fluorescence intensity decreased gradually with increasing CNPs concentration, indicating effective quenching of the protein fluorescence. Figure 2 shows the spectra in the presence of different concentrations of CNPs with Hb and Mb respectively.

Temperature dependent experiment was performed to get the thermodynamic parameters of binding. This experiment showed that quenching constant for CNPs decreased with increasing of temperature. Quenching decreased with increasing temperature, which suggests the static quenching. However, fluorescence lifetime measurements would be a definitive indicator. Binding constants and the thermodynamic parameters[47-48] of the binding are listed in the Table 1. Here we have observed that the entropy of the system increases whereas

enthalpy decreased. Therefore, the process is enthalpy driven. We agree that the entropy change due to adsorption is negative. In this macromolecular system when we consider the contribution of water exclusion/solvent release, the overall entropy of the system increases.[49]

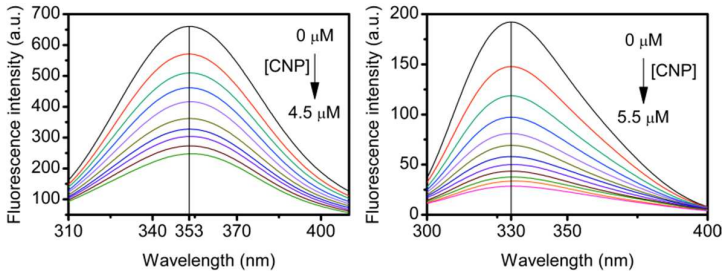

Figure 2 Effect of the compounds on the intrinsic fluorescence of Hb and Mb. (A) The emission spectra of Hb (0.5 μM) as a function of CNPs with concentration varying from 0 μM to 4.5 μM (9 steps). (B) The emission spectra of Mb (0.5 μM) as a function of CNPs with concentration varying from 0 μM to 5.5 μM (11 steps). Emission maximum, 353 nm for Hb and 330 nm for Mb.

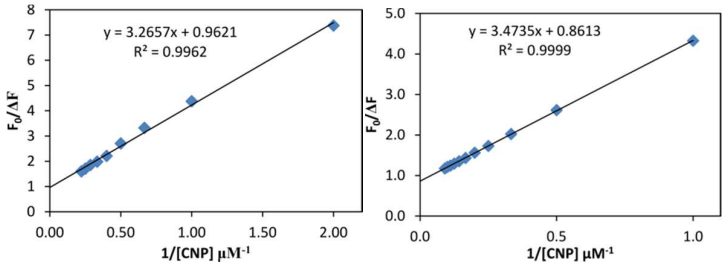

Figure 3 Modified Stern-Volmer plot for the determination of K_d of Hb binding with CNPs (A) and Mb binding with CNPs (B).

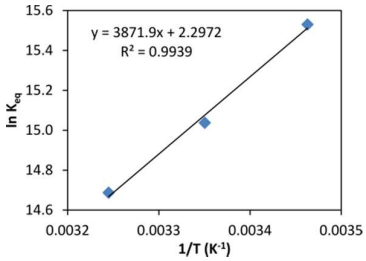

Figure 4 Van't Hoff plot for the determination of thermodynamics parameters of binding of Hb with CNPs.

Table 1 Binding constant and the thermodynamic parameters of binding.

	K_d (μM)	ΔG° (kJ mol^{-1})	ΔH° (kJ mol^{-1})	ΔS° (J mol^{-1} K^{-1})
Hb-CNP	0.29	-37.98	-32.19	19.10
Mb-CNP	0.25	NA	NA	NA

Circular dicroism

Circular dicroism (CD) is a powerful technique to know about the interaction of proteins with other molecules including nanoparticles. Generally this technology is used to determine the protein conformation in solution or adsorbed onto other molecules or nanoparticles. Here the CD spectra were taken in the wavelength range of 200–250 nm by preparing the aliquots of the samples and the results are expressed in the Figure 5.

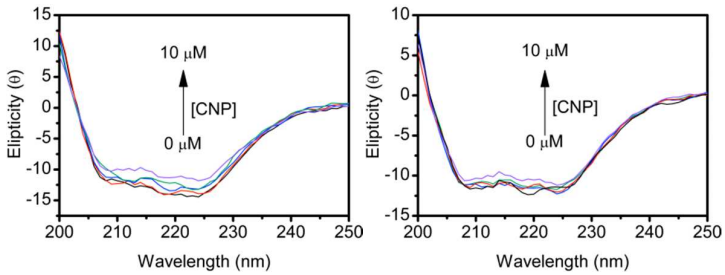

Figure 5 Circular dichroism spectral changes of Hb (A) and Mb (B) on interaction with increasing concentration of CNPs.

The far ultraviolet CD spectra of native Hb and Mb (Figure 5) have two minima at 208 (π–π*) and 223 nm (n–π*), which are characteristic of typical α-helical structure. Carbon nanoparticle is not CD active. For Hb and Mb, changes in the CD spectra for the secondary and tertiary structures have been noted upon CNP binding, but such changes are much greater for Hb than compared to that of Mb. It has been found that binding of CNP to Hb causes a reduction of α-helix of the protein secondary structure from 76% (free Hb) to 61% (Hb-CNP) whereas for Mb the reduction of α-helix of the protein secondary structure from 75% (free Mb) to 71% (Mb-CNP) has been observed. Such results suggest structural changes for both Hb and Mb upon binding to CNP.

Conclusion

The CNPs were synthesized and studied their interactions with Hb and Mb. The results show a remarkably strong interaction between carbon nanoparticles with haemoglobin and myoglobin separately. TEM, AFM and DLS experiments have been performed to confirm the ultrafine nature of the synthesized CNPs. The temperature dependent fluorescence spectroscopy shows the exothermic binding of CNPs to Hb which was favoured by enthalpy and entropy changes. Circular dicroism study also reflects significant disruption of protein secondary structure and partial unfolding of the helical structure. These findings have given information towards the understanding of this strong interaction between carbon nanoparticles with hemoglobin and myoglobin. This might help to better clarify the potential risks and undesirable health hazards of carbon nanoparticles.

References

1. Baxter, J.; Bian, Z.; Chen, G.; Danielson, D.; Dresselhaus, M. S.; Fedorov, A. G.; Fisher, T. S.; Jones, C. W.; Maginn, E.; Kortshagen, U.; Manthiram, A.; Nozik, A.; Rolison, D. R.; Sands, T.; Shi, L.; Sholl, D.; Wu, Y., Nanoscale design to enable the revolution in renewable energy. *Energy & Environmental Science* **2009,** *2* (6), 559-588.

2. Dreaden, E. C.; Alkilany, A. M.; Huang, X.; Murphy, C. J.; El-Sayed, M. A., The golden age: gold nanoparticles for biomedicine. *Chemical Society Reviews* **2012,** *41* (7), 2740-2779.

3. Chen, B.; Jia, Y.; Zhao, J.; Li, H.; Dong, W.; Li, J., Assembled Hemoglobin and Catalase Nanotubes for the Treatment of Oxidative Stress. *The Journal of Physical Chemistry C* **2013**.

4. Wang, T.; Zhang, L.; Su, Z.; Wang, C.; Liao, Y.; Fu, Q., Multifunctional Hollow Mesoporous Silica Nanocages for Cancer Cell Detection and the Combined Chemotherapy and Photodynamic Therapy. *ACS Applied Materials & Interfaces* **2011,** *3* (7), 2479-2486.

5. Kharisov, B. I.; Kharissova, O. V.; Jose-Yacaman, M., Nanostructures with Animal-like Shapes. *Industrial & Engineering Chemistry Research* **2010,** *49* (18), 8289-8309.

6. Long, Y.-Z.; Yu, M.; Sun, B.; Gu, C.-Z.; Fan, Z., Recent advances in large-scale assembly of semiconducting inorganic nanowires and nanofibers for electronics, sensors and photovoltaics. *Chemical Society Reviews* **2012,** *41* (12), 4560-4580.

7. Pattanayak, S.; Priyam, A.; Paik, P., Facile tuning of plasmon bands in hollow silver nanoshells using mild reductant and mild stabilizer. *Dalton Transactions* **2013,** *42* (29), 10597-10607.

8. Banerji, B.; Pramanik, S. K.; Pal, U.; Maiti, N. C., Dipeptide derived from benzylcystine forms unbranched nanotubes in aqueous solution. *Journal of Nanostructure in Chemistry* **2013,** *3* (1), 12.

9. Zhang, Z.; Shao, C.; Li, X.; Wang, C.; Zhang, M.; Liu, Y., Electrospun Nanofibers of p-Type NiO/n-Type ZnO Heterojunctions with Enhanced Photocatalytic Activity. *ACS Applied Materials & Interfaces* **2010,** *2* (10), 2915-2923.

10. Li, H.; Kang, Z.; Liu, Y.; Lee, S.-T., Carbon nanodots: synthesis, properties and applications. *Journal of Materials Chemistry* **2012,** *22* (46), 24230-24253.

11. Lu, X.; Feng, L.; Akasaka, T.; Nagase, S., Current status and future developments of endohedral metallofullerenes. *Chemical Society Reviews* **2012,** *41* (23), 7723-7760.

12. Negishi, Y.; Omata, D.; Iijima, H.; Takabayashi, Y.; Suzuki, K.; Endo, Y.; Suzuki, R.; Maruyama, K.; Nomizu, M.; Aramaki, Y., Enhanced Laminin-Derived Peptide AG73-Mediated Liposomal Gene Transfer by Bubble Liposomes and Ultrasound. *Molecular Pharmaceutics* **2009,** *7* (1), 217-226.

13. Xu, P.; Tan, G.; Zhou, J.; He, J.; Lawson, L. B.; McPherson, G. L.; John, V. T., Undulating Tubular Liposomes through Incorporation of a Synthetic Skin Ceramide into Phospholipid Bilayers. *Langmuir* **2009,** *25* (18), 10422-10425.

14. Liu, C.-M.; Xu, C.; Cheng, Y.; Chen, X.-R.; Cai, L.-C., Size-dependent melting and coalescence of tungsten nanoclusters via molecular dynamics simulation. *Physical Chemistry Chemical Physics* **2013,** *15* (33), 14069-14079.

15. Xu, K.; Cao, P.; Heath, J. R., Achieving the Theoretical Depairing Current Limit in Superconducting Nanomesh Films. *Nano Letters* **2010,** *10* (10), 4206-4210.

16. Reiss, P.; Couderc, E.; De Girolamo, J.; Pron, A., Conjugated polymers/semiconductor nanocrystals hybrid materials-preparation, electrical transport properties and applications. *Nanoscale* **2011,** *3* (2), 446-489.

17. Zhang, Z.; Zeng, X. C.; Guo, W., Fluorinating Hexagonal Boron Nitride into Diamond-Like Nanofilms with Tunable Band Gap and Ferromagnetism. *Journal of the American Chemical Society* **2011,** *133* (37), 14831-14838.

18. Bai, S.; Shen, X., Graphene-inorganic nanocomposites. *RSC Advances* **2012,** *2* (1), 64-98.

19. Horie, M.; Nishio, K.; Fujita, K.; Kato, H.; Nakamura, A.; Kinugasa, S.; Endoh, S.; Miyauchi, A.; Yamamoto, K.; Murayama, H.; Niki, E.; Iwahashi, H.; Yoshida, Y.; Nakanishi,

J., Ultrafine NiO Particles Induce Cytotoxicity in Vitro by Cellular Uptake and Subsequent Ni(II) Release. *Chemical Research in Toxicology* **2009,** *22* (8), 1415-1426.

20. Devadasu, V. R.; Bhardwaj, V.; Kumar, M. N. V. R., Can Controversial Nanotechnology Promise Drug Delivery? *Chemical Reviews* **2012,** *113* (3), 1686-1735.

21. Yan, L.; Zhao, F.; Li, S.; Hu, Z.; Zhao, Y., Low-toxic and safe nanomaterials by surface-chemical design, carbon nanotubes, fullerenes, metallofullerenes, and graphenes. *Nanoscale* **2011,** *3* (2), 362-382.

22. Ge, Z.; Liu, S., Functional block copolymer assemblies responsive to tumor and intracellular microenvironments for site-specific drug delivery and enhanced imaging performance. *Chemical Society Reviews* **2013,** *42* (17), 7289-7325.

23. Ripp, S.; Henry Theodore, B., *Biotechnology and Nanotechnology Risk Assessment: Minding and Managing the Potential Threats around Us*. American Chemical Society: 2011; Vol. 1079, p 0.

24. Petosa, A. R.; Jaisi, D. P.; Quevedo, I. R.; Elimelech, M.; Tufenkji, N., Aggregation and Deposition of Engineered Nanomaterials in Aquatic Environments: Role of Physicochemical Interactions. *Environmental Science & Technology* **2010,** *44* (17), 6532-6549.

25. Arvizo, R. R.; Bhattacharyya, S.; Kudgus, R. A.; Giri, K.; Bhattacharya, R.; Mukherjee, P., Intrinsic therapeutic applications of noble metal nanoparticles: past, present and future. *Chemical Society Reviews* **2012,** *41* (7), 2943-2970.

26. Sharifi, S.; Behzadi, S.; Laurent, S.; Laird Forrest, M.; Stroeve, P.; Mahmoudi, M., Toxicity of nanomaterials. *Chemical Society Reviews* **2012,** *41* (6), 2323-2343.

27. Vollrath, A.; Schubert, S.; Schubert, U. S., Fluorescence imaging of cancer tissue based on metal-free polymeric nanoparticles - a review. *Journal of Materials Chemistry B* **2013,** *1* (15), 1994-2007.

28. United Nations Environment Programme, E. E. A. P., Environmental effects of ozone depletion and its interactions with climate change: progress report, 2009. *Photochemical & Photobiological Sciences* **2010,** *9* (3), 275-294.

29. L. Cao, X. Wang, M.J. Meziani, F. Lu, H. Wang, P.G. Luo, Y. Lin, B.A. Harruff, L.M. Veca, D. Murray, S.Y. Xie, Y.P. Sun, Carbon dots for multiphoton bioimaging, J. Am. Chem. Soc. 129 (2007) 11318–11319.

30. T.W. Kim, P.W. Chung, I.I. Slowing, M. Tsunoda, E.S. Yeung, V.S. Lin, Structurally ordered mesoporous carbon nanoparticles as transmembrane delivery vehicle in human cancer cells, Nano Lett. 8 (2008) 3724–3727.

31. Y.P. Sun, B. Zhou, Y. Lin, W. Wang, K.A. Fernando, P. Pathak, M.J. Meziani, B.A. Harruff, X. Wang, H. Wang, P.G. Luo, H. Yang, M.E. Kose, B. Chen, L.M. Veca, S.Y. Xie, Quantum-sized carbon dots for bright and colorful photoluminescence, J. Am. Chem. Soc. 128 (2006) 7756–7757.

32. Z. Liu, J.T. Robinson, X. Sun, H. Dai, PEGylated nanographene oxide for delivery of water-insoluble cancer drugs, J. Am. Chem. Soc. 130 (2008) 10876–10877.

33. Wang, J.; Velders, A. H.; Gianolio, E.; Aime, S.; Vergeldt, F. J.; Van As, H.; Yan, Y.; Drechsler, M.; de Keizer, A.; Cohen Stuart, M. A.; van der Gucht, J., Controlled mixing of lanthanide(iii) ions in coacervate core micelles. *Chemical Communications* **2013,** *49* (36), 3736-3738.

34. Géhin, E.; Ramalho, O.; Kirchner, S., Size distribution and emission rate measurement of fine and ultrafine particle from indoor human activities. *Atmospheric Environment* **2008,** *42* (35), 8341-8352.

35. Thomas, R. J., Particle size and pathogenicity in the respiratory tract. *Virulence* **2013,** *4* (8), 847-858.

36. Butler, O. T.; Cairns, W. R. L.; Cook, J. M.; Davidson, C. M., Atomic spectrometry update. Environmental analysis. *Journal of Analytical Atomic Spectrometry* **2010,** *25* (2), 103-141.

37. Carter, S.; Fisher, A. S.; Hinds, M. W.; Lancaster, S., Atomic spectrometry update. Industrial analysis: metals, chemicals and advanced materials. *Journal of Analytical Atomic Spectrometry* **2012,** *27* (12), 2003-2053.

38. Khin, M. M.; Nair, A. S.; Babu, V. J.; Murugan, R.; Ramakrishna, S., A review on nanomaterials for environmental remediation. *Energy & Environmental Science* **2012,** *5* (8), 8075-8109.

39. Sapsford, K. E.; Tyner, K. M.; Dair, B. J.; Deschamps, J. R.; Medintz, I. L., Analyzing Nanomaterial Bioconjugates: A Review of Current and Emerging Purification and Characterization Techniques. *Analytical Chemistry* **2011,** *83* (12), 4453-4488.

40. Int Panis, L.; de Geus, B.; Vandenbulcke, G.; Willems, H.; Degraeuwe, B.; Bleux, N.; Mishra, V.; Thomas, I.; Meeusen, R., Exposure to particulate matter in traffic: A comparison of cyclists and car passengers. *Atmospheric Environment* **2010,** *44* (19), 2263-2270.

41. Romieu, I.; Castro-Giner, F.; Kunzli, N.; Sunyer, J., Air pollution, oxidative stress and dietary supplementation: a review. *European Respiratory Journal* **2008,** *31* (1), 179-197.

42. Card, J. W.; Zeldin, D. C.; Bonner, J. C.; Nestmann, E. R., Pulmonary applications and toxicity of engineered nanoparticles. *American Journal of Physiology - Lung Cellular and Molecular Physiology* **2008,** *295* (3), L400-L411.

43. Calderón-Garcidueñas, L.; Solt, A. C.; Henríquez-Roldán, C.; Torres-Jardón, R.; Nuse, B.; Herritt, L.; Villarreal-Calderón, R.; Osnaya, N.; Stone, I.; García, R.; Brooks, D. M.; González-Maciel, A.; Reynoso-Robles, R.; Delgado-Chávez, R.; Reed, W., Long-term Air Pollution Exposure Is Associated with Neuroinflammation, an Altered Innate Immune Response, Disruption of the Blood-Brain Barrier, Ultrafine Particulate Deposition, and

Accumulation of Amyloid β-42 and α-Synuclein in Children and Young Adults. *Toxicologic Pathology* **2008,** *36* (2), 289-310.

44. Jacobs, L.; Nawrot, T.; de Geus, B.; Meeusen, R.; Degraeuwe, B.; Bernard, A.; Sughis, M.; Nemery, B.; Panis, L., Subclinical responses in healthy cyclists briefly exposed to traffic-related air pollution: an intervention study. *Environmental Health* **2010,** *9* (1), 64.

45. Liu, H.; Ye, T.; Mao, C., Fluorescent Carbon Nanoparticles Derived from Candle Soot. *Angewandte Chemie International Edition* **2007,** *46* (34), 6473-6475.

46. Ray, A.; Koley Seth, B.; Pal, U.; Basu, S., Nickel(II)-Schiff base complex recognizing domain II of bovine and human serum albumin: Spectroscopic and docking studies. *Spectrochimica Acta Part A: Molecular and Biomolecular Spectroscopy* **2012,** *92* (0), 164-174.

47. Banerjee, M.; Pal, U.; Subudhhi, A.; Chakrabarti, A.; Basu, S., Interaction of Merocyanine 540 with serum albumins: Photophysical and binding studies. *Journal of Photochemistry and Photobiology B: Biology* **2012,** *108* (0), 23-33.

48. Banerji, B.; Pramanik, S.; Pal, U.; Maiti, N., Potent anticancer activity of cystine-based dipeptides and their interaction with serum albumins. *Chemistry Central Journal* **2013,** *7* (1), 9143.

49. Schmid, M. J.; Bickel, K. R.; Novák, P.; Schuster, R., Microcalorimetric Measurements of the Solvent Contribution to the Entropy Changes upon Electrochemical Lithium Bulk Deposition. *Angewandte Chemie International Edition* **2013,** *52* (50), 13233-13237.

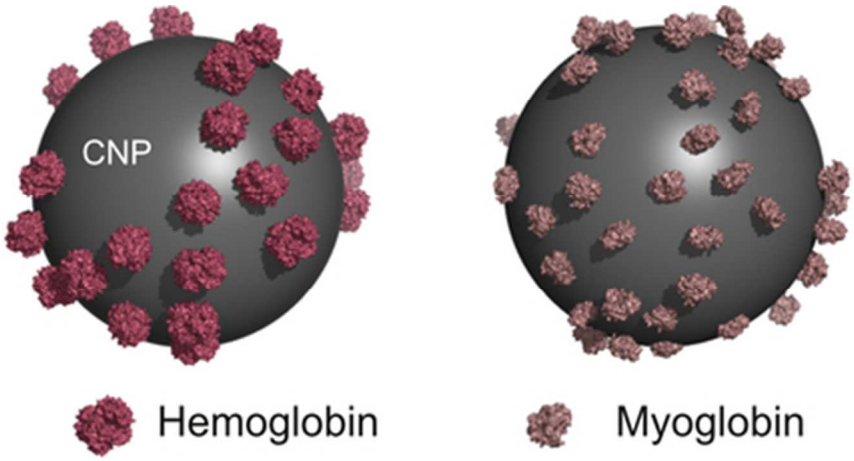

Binding of hemoglobin and myoglobin to carbon nanoparticles:
39x19mm (300 x 300 DPI)